Journal of Advanced Ceramics
2017, **6**(1): 43–49
DOI: 10.1007/s40145-016-0216-y

ISSN 2226-4108
CN 10-1154/TQ

Research Article

Electronic structures and optical properties of monoclinic ZrO_2 studied by first-principles local density approximation + *U* approach

Jinping LI[a,c,*], Songhe MENG[a], Jiahong NIU[a], Hantao LU[b,c]

[a]*Center for Composite Materials and Structures*, *Harbin Institute of Technology*, *Harbin 150080*, *China*
[b]*Center for Interdisciplinary Studies & Key Laboratory for Magnetism and Magnetic Materials of the MoE*, *Lanzhou University*, *Lanzhou 730000*, *China*
[c]*Yukawa Institute for Theoretical Physics*, *Kyoto University*, *Kyoto*, *606-8502*, *Japan*

Received: May 09, 2016; Revised: November 25, 2016; Accepted: December 16, 2016

Abstract: The electronic structures and optical properties of the monoclinic ZrO_2 (m-ZrO_2) are investigated by means of first-principles local density approximation (LDA) + *U* approach. Without on-site Coulomb interactions, the band gap of m-ZrO_2 is 3.60 eV, much lower than the experimental value (5.8 eV). By introducing the Coulomb interactions of 4d orbitals on Zr atom (U^d) and of 2p orbitals on O atom (U^p), we can reproduce the experimental value of the band gap. The calculated dielectric function of m-ZrO_2 exhibits a small shoulder at the edge of the band gap in its imaginary part, while in the tetragonal ZrO_2 and cubic ZrO_2 it is absent, which is consistent with the experimental observations. The origin of the shoulder is attributed to the difference of electronic structures near the edge of the valence and conduction bands.

Keywords: monoclinic ZrO_2 (m-ZrO_2); first-principles; local density approximation (LDA) + *U*; electronic structure; optical properties

1 Introduction

ZrO_2 is widely studied both experimentally and theoretically because of its excellent dielectric properties, wide band gap, high melting point, etc. [1,2]. Moreover, ZrO_2 has been proven to have one of the most high dielectric constants [3] and be promising in optical and protective coatings [4,5].

ZrO_2 exists in three polymorphs at atmospheric pressure [6]: the monoclinic, the tetragonal, and the cubic fluorite, denoted as m-, t-, and c-ZrO_2, respectively. It has been known that the electronic structures and optical properties of the thermally annealed samples depend on their preparation process and the resulting structural details. In the thin films of ZrO_2 after annealing at 900 ℃, a small shoulder at the threshold of the absorption spectra has been detected [7]. The same characteristic appears in the dielectric function of as-deposited ZrO_2 films of 9.9 and 5.3 nm after rapid thermal anneals (RTA) at 600 ℃ [8]. On the other hand, no shoulder structure has been observed in both tetragonal phase and cubic phase. The exact reason about the small shoulder is still unclear. Therefore, it is essential to investigate the electronic structure of ZrO_2 and clarify the relations between the optical properties and lattice structures from the first-principles calculations.

The band structures of m-ZrO_2 have been calculated by taking into account spin-orbit interactions within the

* Corresponding author.
E-mail: lijinping@hit.edu.cn

framework of local density approximation (LDA) and general gradient approximation (GGA) [9]. The resulting band gap is about 3.58 eV, smaller than the experimental value, 5.8 eV [3]. The modified band structures incorporating the effect of electron correlations have been obtained by the *GW* approximation, giving rise to the band gap value of 5.34 eV, much closer to the experimental one. However, the *GW* calculation costs a lot in terms of numerical demands [10]. Another technique to include correlation effect with less computational effort is the so-called LDA + U or GGA + U approach [11,12]. The LDA (GGA) + U approach can give a qualitative improvement compared with the LDA (GGA) [11–13]. Further LDA + U^{f} + U^{p}, LDA + U^{d} + U^{p}, and GGA + U^{d} + U^{p} have been used for the description of CeO_2, monoclinic HfO_2, and cubic HfO_2, respectively, leading to improved descriptions of the electronic structures [14–16]. Therefore, it is reasonable to use the approach for the investigation of m-ZrO_2.

In this paper, we use the LDA + U scheme formulated by Loschen *et al.* [17], to calculate the electric structures and optical properties of m-ZrO_2. The on-site Coulomb interactions of 4d orbitals on Zr atom (U^{d}) and of 2p orbitals on O atom (U^{p}) are determined so as to reproduce the experimental value of band gap for m-ZrO_2. The calculated imaginary part of the dielectric function exhibits a shoulder structure at the edge of the band gap. Such a shoulder is absent in t-ZrO_2 and c-ZrO_2, well agreeing with experimental results. The origin of the shoulder is attributed to the difference of the electronic structures near the edge of the valence and conduction bands. In our former paper [15], we have predicted that similar to m-HfO_2, a small shoulder can also be found in the optical absorption of m-ZrO_2. Here explicitly numerical evidence is provided.

2 Computational methodology

Density functional theory (DFT) calculations are performed with plane-wave ultrasoft pseudopotential, by using the LDA with CA-PZ functional and the LDA + U approach as implemented in the CASTEP (Cambridge Sequential Total Energy Package) code [18]. The ionic cores are represented by ultrasoft pseudopotentials for Zr and O atoms. For Zr atom, the configuration is [Kr] $4d^2 5s^2$, where the $4s^2$, $4p^6$, $4d^2$, and $5s^2$ electrons are explicitly treated as valence electrons. For O atom, the configuration is [He] $2s^2 2p^4$, where $2s^2$ and $2p^4$ electrons are explicitly treated as valence electrons. The plane-wave cut off energy is 380 eV and the Brillouin-zone integration is performed over the 6 × 6 × 6 grid sizes using the Monkorst–Pack method for monoclinic structure optimization. This set of parameters assures the total energy convergence of 5.0×10^{-6} eV/atom, the maximum force of 0.01 eV/Å, the maximum stress of 0.02 GPa, and the maximum displacement of 5.0×10^{-4} Å. We calculate the electronic structures and optical properties of m-ZrO_2 by means of LDA without U and LDA + U^{d} + U^{p} after having optimized the geometry structure. The details of the calculation will be shown elsewhere [16].

3 Results and discussion

The space group of m-ZrO_2 is $P2_1/c$ and the local symmetry is C_{2h}^5. The lattice constants a, b, c, and β is experimentally determined to be $a = 0.5145$ nm, $b = 0.5208$ nm, $c = 0.5311$ nm, and $\beta = 99.2°$. The LDA calculation of the perfect bulk m-ZrO_2 is performed to determine the optimized parameters in order to check the applicability and accuracy of the ultrasoft pseudopotential. The optimized parameters are $a = 0.5087$ nm, $b = 0.5175$ nm, $c = 0.5249$ nm, and $\beta = 99.6°$, in good agreement with experimental [19] and other theoretical values [6,9,20]. However, the value of the band gap E_{g} is around 3.60 eV, much smaller than the experimental value of 5.8 eV [3]. This is due to the fact that the DFT results often undervalue the energy of 4d orbitals on Zr atom, lowering the bottom level of conduction bands.

In order to reproduce the band gap, we first introduce U^{d} for 4d orbitals on Zr atom. Using the experimental lattice parameters, we optimize geometry structure and calculate the band structure and density of states (DOS) of m-ZrO_2. The band gap E_{g} obtained from the band structure as a function of U^{d} is shown in Fig. 1(a). It can be seen that E_{g} firstly increases and then drops with increasing U^{d}, showing a maximum value (4.93 eV) at $U^{\mathrm{d}} = 11.0$ eV, where the lattice parameters of the optimized structure are $a = 0.5335$ nm, $b = 0.5201$ nm, $c = 0.5418$ nm, and $\beta = 98.8°$. The maximum value is smaller than the experimental one (5.8 eV). The saturation of E_{g} with U^{d} may be related to the approach of 4d states toward 5s and 5p states, though microscopic mechanism is not yet fully

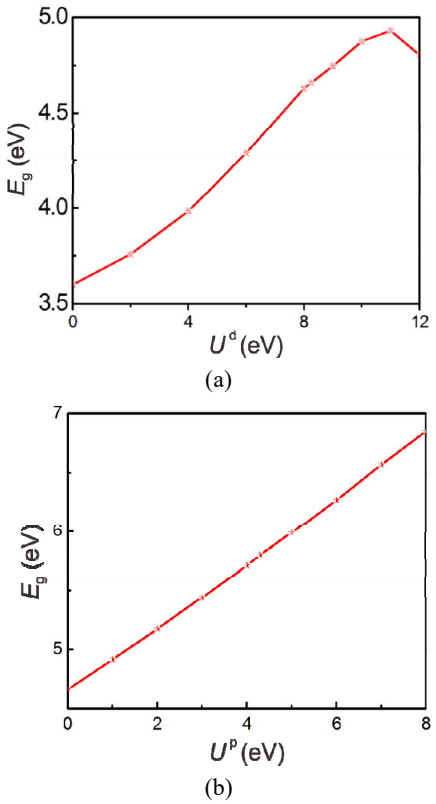

Fig. 1 Calculated band gap E_g as a function of (a) U^d and (b) U^p while $U^d = 8.0$ eV.

understood. Next, we introduce U^p for 2p orbitals on O atom, while keeping $U^d = 8.0$ eV unchanged. The results in Fig. 1(b) show that E_g monotonically increases with U^p. When $U^d = 8.0$ eV and $U^p = 4.35$ eV, the calculated band gap of m-ZrO_2 is 5.8 eV, well coinciding with experiment. The lattice parameters of the optimized structure here are $a = 0.5237$ nm, $b = 0.5145$ nm, $c = 0.5355$ nm, and $\beta = 99.2°$.

The reason for adopting $U^d = 8.0$ eV is based on the following arguments. First, note that when U^d value is 11.0 eV, where the band gap reaches its maximum, the lattice parameter β is less than 90°, which indicates the occurrence of a lattice distortion in the m-ZrO_2 cell. Secondly, based on our previous results for the monoclinic HfO_2 (m-HfO_2), where the optimal value of U^d for Hf atoms is 8.0 eV [15], we expect that the U^d value for Zr atoms might be close to 8.0 eV as well. In Fig. 2, we further depict the evolution of the imaginary part ε_2 with the changes of U^d for Zr atoms and of U^p for O atoms. From Fig. 2(a), we can see that the behavior of ε_2 undergoes a conceivable change around $U^d = 8.0$ eV. On the other hand, at the fixed $U^d = 8.0$ eV, the development of ε_2 with the change of U^p, as shown in Fig. 2(b), is quite smooth.

Besides, we present the calculations about the volume modulus of m-ZrO_2 changed with U^d, and with U^p while fixing $U^d = 8.0$ eV in Fig. 3. From Fig. 3(a), it can be seen that the volume modulus changes non-monotonically with the increase of U^d. The two turning points are around 2 and 10 eV. We suggest that the reasonable values for U^d could be 2 eV $\leqslant U^d \leqslant$ 10 eV. On the other hand, as shown in Fig. 3(b), with the increase of U^p ($U^d = 8.0$ eV), the volume modulus experiences abrupt change after above 4.4 eV; while before 4.4 eV, it is almost flat. At $U^d = 8.0$ eV and $U^p = 4.35$ eV, the theoretical value of the bulk modulus obtained by LDA + U is 188.43 GPa, well agreeing with the experimental value 189 GPa in Ref. [21].

It should be noted that there exist different combinations of U^d and U^p which may reproduce the band gap value as well. For example, when $U^d = 11.0$ eV, $U^p = 3.2$ eV, the resulting E_g is 5.807 eV; $U^d = 8.25$ eV and $U^p = 4.25$ eV give $E_g = 5.802$ eV. It has been checked that these values produce similar electronic structures and optical properties. Based on the above arguments, and the reference to other numerical results,

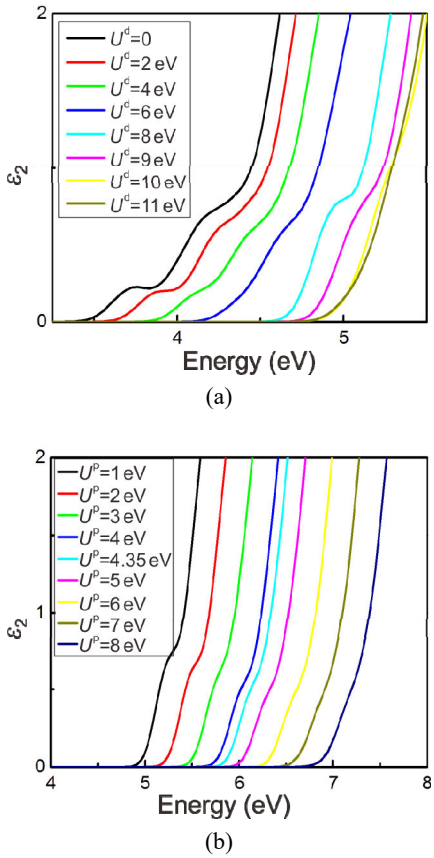

Fig. 2 Evolution of the imaginary part of the dielectric function with (a) U^d and (b) U^p while $U^d = 8.0$ eV.

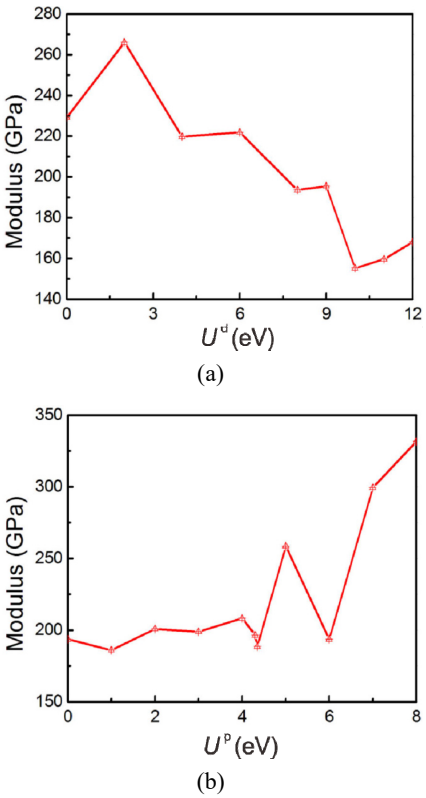

Fig. 3 Volume modulus of m-ZrO_2 changed with (a) U^d and (b) U^p while $U^d = 8.0$ eV.

we choose $U^d = 8.0$ eV, $U^p = 4.35$ eV as a typical representative.

By adopting these U values ($U^d = 8.0$ eV and $U^p = 4.35$ eV), we perform the LDA + U calculation. The band dispersion is shown in Fig. 4(a). The bottom of the conduction band is located at the G/B point. Since the bottom shifts to higher energy with U^d, accompanied by the reconstruction of the conduction band, the separated DOS at 5.6 and 8.7 eV obtained by LDA without U (not shown) merge to one sharp structure at 6.9 eV in Fig. 4(b). The conduction band is predominantly constructed by Zr 4d states, while the valence band is by O 2p states, as shown in Fig. 4(c) and Fig. 4(d), respectively. Therefore, the excitation across the gap is from the O 2p states to the Zr 4d states.

Figure 5(a) shows the real part ε_1 and the imaginary part ε_2 of the dielectric function of m-ZrO_2 obtained by LDA and LDA + U^d + U^p, where we can see that the difference between these two methods mainly comes from the position shifts of the curves due to the enlargement of the band gap by LDA + U^d + U^p. The small shoulder in the imaginary part of the dielectric function persists by either LDA or LDA + U^d + U^p. This

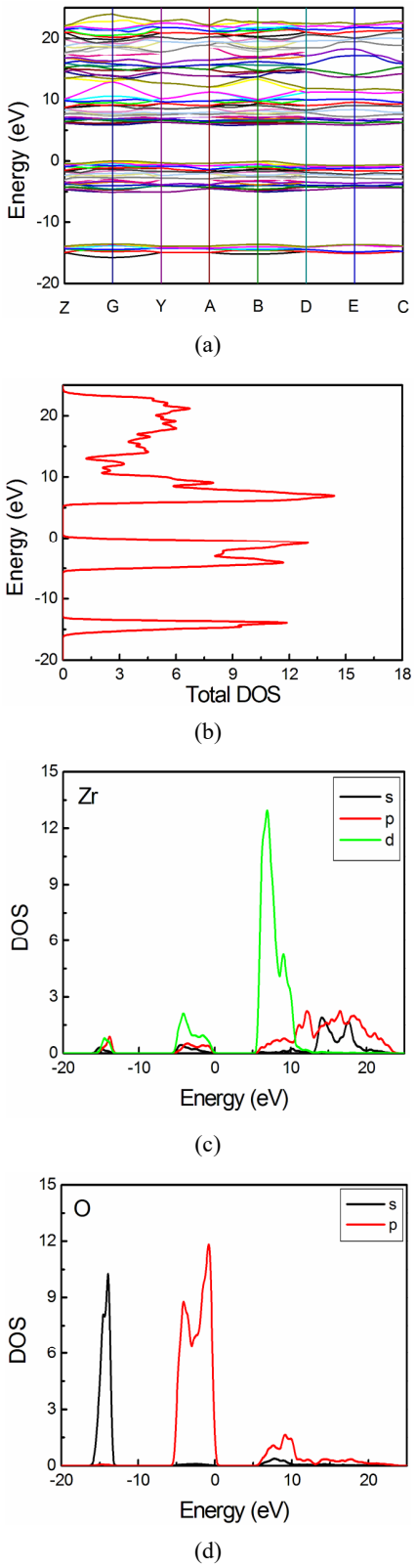

Fig. 4 Band structure and density of states (DOS) of m-ZrO_2 calculated by use of LDA + U^d (8.0 eV) + U^p (4.35 eV). (a) Band structure, (b) total DOS, (c) partial DOS of Zr atom, and (d) partial DOS of O atom.

implies the robustness of the small shoulder in m-ZrO_2, similar to m-HfO_2 [15]. The calculated static dielectric constant is 3.98 by LDA + U^d + U^p (5.34 by LDA without U), coinciding with the experimental value 4.10 [22]. The imaginary part ε_2 shows a maximum at 9.83 eV. The maximum value (~7.99) is very close to the other theoretical value (~8.0) [9], in contrast with the value by the LDA without U (~9.78, not shown). Other optical properties can be computed from the complex dielectric function [23]. We obtain the refractive coefficient n = 1.99 of m-ZrO_2 by LDA + U^d + U^p (2.31 by LDA without U), which is close to the experimental value (n = 2.07 [24], 2.04 [25], and 1.932 [26]).

Additional information is provided in Fig. 5(b) where the dielectric functions of m-ZrO_2 and m-HfO_2 obtained by LDA + U^d + U^p approach are shown. Similar shoulder structures at the edge of the absorption spectra can be found in the monoclinic phases of the two materials.

To further build up the connection between the emergence of the shoulder structure in the optical spectrum and the underlying lattice structure, in Fig. 6(a), the imaginary parts of complex dielectric functions for m-, t-, and c-ZrO_2 by LDA + U^d + U^p are shown. The values of U^d and U^p for both phases are chosen so that the experimental gap values can be reproduced: U^d = 8.25 eV (8.25 eV) and U^p = 5.0 eV (4.6 eV) for t-ZrO_2 (c-ZrO_2). We find similar spectra between t-ZrO_2 and c-ZrO_2 with only a small shift (~1 eV) of the position; while not only the global spectral distribution but also the spectral weight at the edge of the band gap in ε_2 show a significant contrast between m-ZrO_2 and t-ZrO_2. As shown in the inset of Fig. 6(a), different from t- or c-ZrO_2, a clear shoulder structure can be found at the edge of the band gap (~6.0 eV) in m-ZrO_2.

In order to understand the origin of the shoulder, we show in Fig. 6(b) the comparison of the total DOS between m-ZrO_2, t-ZrO_2, and c-ZrO_2. We find that for both valence and conduction bands, the DOS in t-ZrO_2 and c-ZrO_2 are similar, while the DOS in m-ZrO_2 is quite different from them. In particular, at the edge of

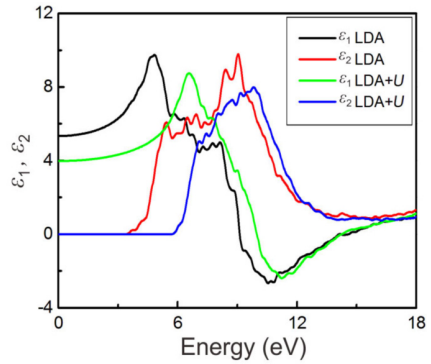

(a)

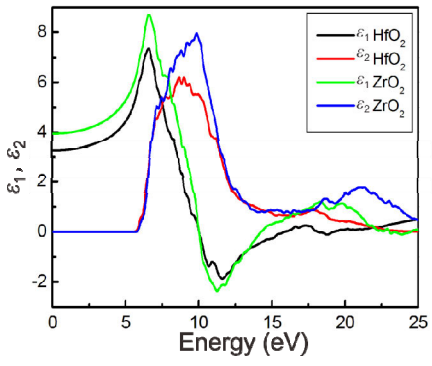

(b)

Fig. 5 (a) Dielectric function for m-ZrO_2 by LDA without U and LDA + U^d + U^p; (b) comparison of m-ZrO_2 and m-HfO_2 calculated by LDA + U^d + U^p.

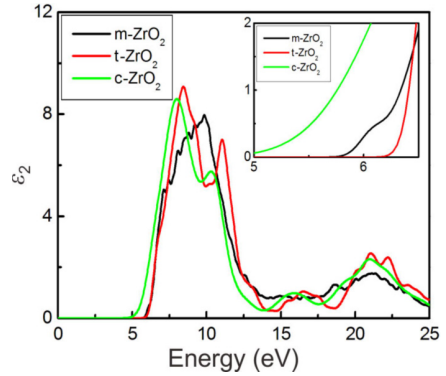

(a)

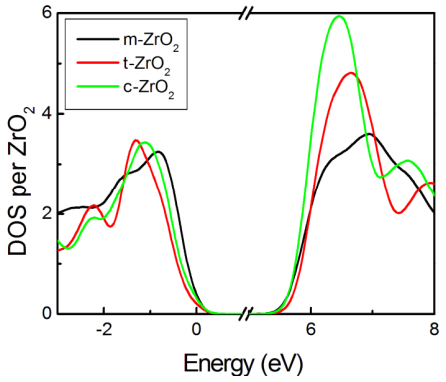

(b)

Fig. 6 Difference of (a) dielectric function and (b) total DOS between m-ZrO_2 and t(c)-ZrO_2 calculated by LDA + U^d + U^p. In (a), the imaginary parts ε_2 of the dielectric functions for m-ZrO_2, t-ZrO_2, and c-ZrO_2 are shown in black, red, and green lines, respectively. The inset displays the fine structure of ε_2 near the gap edge. In (b), the DOS per ZrO_2 is plotted.

the valence band, the DOS in m-ZrO_2 smoothly increases but there is a step feature in t-ZrO_2 and c-ZrO_2 at the edge instead. Furthermore, the conduction band in m-ZrO_2 shows a broad feature of DOS around 6.5 eV. In contrast, in t-ZrO_2 and c-ZrO_2, a peak appears near 6 eV. Since for band insulators, ε_2 is basically given by the cross-band excitations, the difference of DOS between m-ZrO_2 and t(c)-ZrO_2 is indicative of the exclusive presence of the shoulder in ε_2 for m-ZrO_2. A more detailed microscopic origin of the shoulder, such as the assignment of the momentum and band index, remains to be solved in the future. We note that the shoulder structure also appears at the edge of the band gap in the standard LDA calculation without U, as shown in Fig. 5(a). This could mean that the reconstruction of the electronic states due to the monoclinic structure is crucial for the shoulder structure.

The experimental studies for HfO_2 have shown that HfO_2 films reveal a shoulder-like feature in ε_2 [27–29]. But the experimental data of ZrO_2 films does not show a similar shoulder [30,31]. In many aspects, ZrO_2 resembles its twin oxide, HfO_2, though it is generally believed that the electron correlations in ZrO_2 are weaker. In our results, the shoulder-like feature in the dielectric function is also identified in the monoclinic phase of ZrO_2, which on the other hand is absent in the other two phases (tetragonal and cubic). It is consistent with other theoretical results, e.g., the one obtained by full-relativistic calculation [9]. Here we would like to point out that in order to prepare pristine crystallized ZrO_2 with monoclinic structure, the temperature of thermal annealing should reach over 900 ℃ [7] or even higher to 1000 ℃ [32], or prepare as-deposited ZrO_2 films of 9.9 and 5.3 nm after RTA at 600 ℃ [8]. It seems to indicate that for the ZrO_2 samples used in the optical measurements, the monoclinic component may not be dominant. If the monoclinic ZrO_2 (m-ZrO_2) is prevalent in the mixture of the three phases [7,8], the shoulder-like structure should appear in the imaginary part of the dielectric function.

4 Conclusions

In summary, the on-site Coulomb interactions have been introduced for 4d orbitals on Zr atom (U^{d}) and 2p orbitals on O atom (U^{p}) of m-ZrO_2 in the first-principles LDA band structure calculation. The optimal values of U^{d} and U^{p} which can reproduce the experimental value of band gap are obtained. The electron structures and optical properties of m-ZrO_2 are calculated accordingly. We find a shoulder structure at the edge of the band gap in the imaginary part of the dielectric function, consistent with the experimental observation in the crystalline samples of m-ZrO_2. We have also confirmed that such a shoulder is absent in t-ZrO_2 and c-ZrO_2. The origin of the shoulder is attributed to the difference of electronic structures near the edge of the valence and conduction bands between m-ZrO_2 and t(c)-ZrO_2.

Acknowledgements

This work was supported by the National Natural Science Foundation of China (Grant Nos. 11121061 and 11672087), the Strategic Programs for Innovative Research (SPIRE), the Computational Materials Science Initiative (CMSI), and the Yukawa International Program for Quark-Hadron Sciences at YITP, Kyoto University.

References

[1] Cabello G, Lillo L, Caro C, *et al*. Structure and optical characterization of photochemically prepared ZrO_2 thin films doped with erbium and europium. *J Non-Cryst Solids* 2008, **354**: 3919–3928.

[2] Dash LK, Vast N, Baranek P, *et al*. Electronic structure and electron energy-loss spectroscopy of ZrO_2 zirconia. *Phys Rev B* 2004, **70**: 245116.

[3] Houssa M, Afanas'ev VV, Stesmans A, *et al*. Variation in the fixed charge density of SiO_x/ZrO_2 gate dielectric stacks during postdeposition oxidation. *Appl Phys Lett* 2000, **77**: 1885–1887.

[4] Wang SJ, Ong CK, Xu SY, *et al*. Crystalline zirconia oxide on silicon as alternative gate dielectrics. *Appl Phys Lett* 2001, **78**: 1604–1606.

[5] Lin Y-S, Puthenkovilakam R, Chang JP, *et al*. Interfacial properties of ZrO_2 on silicon. *J Appl Phys* 2003, **93**: 5945–5952.

[6] French RH, Glass SJ, Ohuchi FS, *et al*. Experimental and theoretical determination of the electronic structure and optical properties of three phases of ZrO_2. *Phys Rev B* 1994, **49**: 5133–5142.

[7] Lucovsky G, Hong JG, Fulton CC, *et al*. Conduction band states of transition metal (TM) high-*k* gate dielectrics as determined from X-ray absorption spectra. *Microelectron Reliab* 2005, **45**: 827–830.

[8] Sayan S, Nguyen NV, Ehrstein J, *et al*. Structural, electronic, and dielectric properties of ultrathin zirconia films on silicon. *Appl Phys Lett* 2005, **86**: 152902.

[9] Garcia JC, Scolfaro LMR, Lino AT, *et al*. Structural, electronic, and optical properties of ZrO_2 from *ab initio*

calculations. *J Appl Phys* 2006, **100**: 104103.
[10] Jiang H, Gomez-Abal RI, Rinke P, *et al*. Electronic band structure of zirconia and hafnia polymorphs from the *GW* perspective. *Phys Rev B* 2010, **81**: 085119.
[11] Anisimov VI, Aryasetiawan F, Lichtenstein AI. First-principles calculations of the electronic structure and spectra of strongly correlated systems: the LDA + *U* method. *J Phys: Condens Matter* 1997, **9**: 767–808.
[12] Sun B, Zhang P. First-principles local density approximation (LDA) + *U* and generalized gradient approximation (GGA) + *U* studies of plutonium oxides. *Chinese Phys B* 2008, **17**: 1364–1370.
[13] Zhang Y, Jiang H. Intra- and interatomic spin interactions by the density functional theory plus *U* approach: A critical assessment. *J Chem Theory Comput* 2011, **7**: 2795–2803.
[14] Plata JJ, Márquez AM, Sanz JF. Communication: Improving the density functional theory + *U* description of CeO_2 by including the contribution of the O 2*p* electrons. *J Chem Phys* 2012, **136**: 041101.
[15] Li J, Han J, Meng S, *et al*. Optical properties of monoclinic HfO_2 studied by first-principles local density approximation + *U* approach. *Appl Phys Lett* 2013, **103**: 071916.
[16] Li J, Meng S, Li L, *et al*. First-principles generalized gradient approximation (GGA) + $U^d + U^p$ studies of electronic structures and optical properties in cubic HfO_2. *Comp Mater Sci* 2014, **81**: 397–401.
[17] Loschen C, Carrasco J, Neyman KM, *et al*. First-principles LDA + *U* and GGA+*U* study of cerium oxides: Dependence on the effective *U* parameter. *Phys Rev B* 2007, **75**: 035115.
[18] Segall MD, Lindan PJD, Probert MJ, *et al*. First-principles simulation: Ideas, illustrations and the CASTEP code. *J Phys: Condens Matter* 2002, **14**: 2717.
[19] Rignanese G-M. Dielectric properties of crystalline and amorphous transition metal oxides and silicates as potential high-κ candidates: The contribution of density-functional theory. *J Phys: Condens Matter* 2005, **17**: R357.
[20] Walter EJ, Lewes SP, Rappe AM. First principles study of carbon monoxide adsorption on zirconia-supported copper. *Surf Sci* 2001, **495**: 44–50.
[21] Nevitt MV, Chan S-K, Liu JZ, *et al*. The elastic properties of monoclinic ZrO_2. *Physica B+C* 1988, **150**: 230–233.
[22] Camagni P, Samoggia G, Sangaletti L, *et al*. X-ray-photoemission spectroscopy and optical reflectivity of yttrium-stabilized zirconia. *Phys Rev B* 1994, **50**: 4292.
[23] Wang J, Li HP, Stevens R. Hafnia and hafnia-toughened ceramics. *J Mater Sci* 1992, **27**: 5397–5430.
[24] Wang B-Y, Yuan X-D, Jiang X-D, *et al*. the optical properties of SiO_2 and ZrO_2 films investigated by spectroscopic ellipometry. *Piezoelectrics & Acoustooptics* 2008, **39**: 747–750.
[25] Kappertz SVO, Weis H, Wuttig RDRJM. Structural and optical properties of thin zirconium oxide films prepared by reactive direct current magnetron sputtering. *J Appl Phys* 2002, **92**: 3599–3607.
[26] Martin PJ, Netterfield RP, Sainty WG. Modification of the optical and structural properties of dielectric ZrO_2 films by ion-assisted deposition. *J Appl Phys* 1984, **55**: 235–241.
[27] Park J-W, Lee D-K, Lim D, *et al*. Optical properties of thermally annealed hafnium oxide and their correlation with structural change. *J Appl Phys* 2008, **104**: 033521.
[28] Aarik J, Mändar H, Kirm M, *et al*. Optical characterization of HfO_2 thin films grown by atomic layer deposition. *Thin Solid Films* 2004, **466**: 41–47.
[29] Bharathi KK, Kalidindi NR, Ramana CV. Grain size and strain effects on the optical and electrical properties of hafnium oxide nanocrystalline thin films. *J Appl Phys* 2010, **108**: 083529.
[30] Shin HC, Son LS, Kim KR, *et al*. Band alignment and optical properties of $(ZrO_2)_{0.66}(HfO_2)_{0.34}$ gate dielectrics thin films on p-Si (100). *J Surf Anal* 2010, **17**: 203–207.
[31] Lin Y-S, Puthenkovilakam R, Chang JP, *et al*. Interfacial properties of ZrO_2 on silicon. *J Appl Phys* 2003, **93**: 5945–5952.
[32] Tang J, Zhang F, Zoogman P, *et al*. Martensitic phase transformation of isolated HfO_2, ZrO_2, and $Hf_xZr_{1-x}O_2$ ($0 < x < 1$) nanocrystals. *Adv Funct Mater* 2005, **15**: 1595–1602.